HHS Public Access

Author manuscript

Nano Today. Author manuscript; available in PMC 2018 October 16.

Published in final edited form as:

Nano Today. 2016 December ; 11(6): 778–792. doi:10.1016/j.nantod.2016.10.006.

Microfluidic Hydrodynamic Focusing for Synthesis of Nanomaterials

Mengqian Lu[a,+], **Adem Ozcelik**[a,+], **Christopher L. Grigsby**[b,c], **Yanhui Zhao**[a], **Feng Guo**[a], **Kam W. Leong**[b,c,*], and **Tony Jun Huang**[a,*]

[a]Department of Engineering Science and Mechanics, The Pennsylvania State University, University Park, PA, 16802, USA

[b]Department of Biomedical Engineering, Duke University, Durham, North Carolina, 27708, USA

[c]Departments of Biomedical Engineering, and Systems Biology, Columbia University, New York, New York, 10027, USA

Abstract

Microfluidics expands the synthetic space such as heat transfer, mass transport, and reagent consumption to conditions not easily achievable in conventional batch processes. Hydrodynamic focusing in particular enables the generation and study of complex engineered nanostructures and new materials systems. In this review, we present an overview of recent progress in the synthesis of nanostructures and microfibers using microfluidic hydrodynamic focusing techniques. Emphasis is placed on distinct designs of flow focusing methods and their associated mechanisms, as well as their applications in material synthesis, determination of reaction kinetics, and study of synthetic mechanisms.

Graphical Abstract

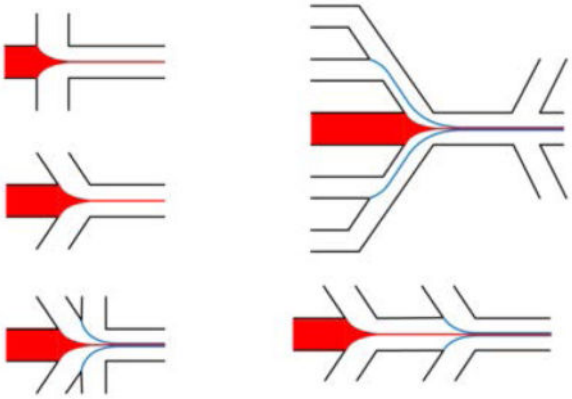

[+]These authors contributed equally to this work.

Keywords

Microfluidics; Hydrodynamic focusing; Nanomaterials synthesis

1. Introduction

Microfluidic devices, which handle fluids with volumes typically ranging from microliters to picoliters, have spawned important applications in many research fields including biology, medicine, chemistry, and engineering sciences [1–5]. On these microscopic scales, the fluid behavior is primarily influenced by viscosity rather than inertia, and the ratio of surface area to volume becomes larger providing rapid heat and mass transfer [6]. These intrinsic properties make microfluidic techniques effective tools for applications such as chemical synthesis, study of reaction kinetics, biological sample preparation, and chemical and biological analyte detection [7]. As micro- and nano-fabrication techniques have matured, using microfluidic tools for synthesis has become more attractive with advantages of product uniformity, small footprint, precise control over reactions, and safer operation compared to large-scale reactors.

In the past several decades, a diverse range of microfluidic reactors have been designed for synthesis of a variety of functional materials [8]. Continuous-flow, droplet-based and digital microfluidics have been applied to produce materials with sizes ranging from nanometers to hundreds of micrometers, which have been considered broadly in several review papers [8–14]. Hydrodynamic focusing (HF) techniques are classified as continuous-flow microfluidics. Relative to droplet-based techniques, HF is straightforward to implement, and simple to simulate and understand because it is pure hydrodynamics that includes the surface tension effects at the liquid-liquid interface without the necessity of considering surface tension effects at the liquid-gas interface. HF techniques can accommodate high flow rates, rendering high-throughput applications possible. HF also enables highly controllable operational conditions owing to the fact that the flow behavior is the most influential parameter for synthesis and can be precisely controlled through varying flow rates. In fact, HF has been utilized for biological research long before the term “microfluidics” was coined. For example, commercial flow cytometers utilize HF for high-throughput single-cell analysis. Given the recent growth of research studies on materials synthesis by HF techniques, we focus this review on the advantages and challenges of this technique for materials synthesis, and to examine whether it is mature enough for industrial and clinic implementation or if there are further steps to be taken.

In this review, we outline the working principles of HF devices, describe materials synthesized through microfluidic HF techniques, and detail the applications in studies of reaction kinetics and synthesis mechanisms. Then, we compare HF technique with other microfluidic synthesis techniques, consider the advantages and limitations, and discuss the potential for HF techniques in the future.

2. Hydrodynamic focusing (HF) devices

Unlike macroscale fluid flow, which is generally turbulent, the flow in microfluidic channels falls into the laminar regime. In turbulent flow, inertial forces are dominant, while in laminar flow, the viscous forces are more prominent. Reynolds number (Re) is a measure of the ratio between inertial forces to viscous forces [15]:

$$Re = \rho u L/\mu$$

where ρ is the fluid density, u is the mean fluid velocity and μ is the dynamic viscosity. Here L is the hydraulic diameter of the channel, which can be expressed by:

$$L = 4A/P_{wet}$$

where A is the channel cross-section area and P_{wet} is wetted perimeter.

In microfluidic channels, Re is generally less than 100, indicative of a laminar flow regime. For some extreme cases, Re can be higher indicating the flow is turbulent in a microfluidic channel [16]. The laminar flow profile creates two effects. First, the fluid velocity distribution depends on the boundary conditions which results in a parabolic distribution of fluid velocity in a pressure driven flow (Figure 1a). Second, there is no turbulence and the mass transfer depends purely on diffusion. Given the latter, the average mixing time τ_{mix} can be calculated using the following equation:

$$\tau_{mix} \propto x^2/D$$

where x is the diffusion length (the distance that the solute needs to travel during the diffusion), and D is the diffusion coefficient. In low Re microfluidic systems, various mixing mechanisms have been demonstrated [17] using active approaches, such as magnetic [18,19], electrokinetic [20], acoustic [21–23], optical based [24] as well as passive approaches such as tesla microstructures [25,26], serpentine channels [27], and lamination [28]. These approaches either require an external mechanism to induce mixing or lacks the dynamic control of the fluid interface.

In the basic HF process, a central solution with a lower flow rate flows within an outer sheath fluid with a higher flow rate, enabling the compression of the central flow [29,30]. This compression decreases mixing times significantly by reducing the required diffusion length [31,32]. Reduced mixing time can improve the quality of synthesized products, such as nanoparticles, which are normally synthesized through bottom-up approaches involving condensation of molecular matter dissolved in liquid [33,34]. This process is triggered either by increasing the solute concentration or decreasing the solubility which results in formation of nuclei [35]. By controlling the relative flow rates of the chemical components, the concentration and solubility can be controlled, which in turn determines the size of the growing nuclei [36,37]. When the reaction is confined within a focused central flow away from the channel walls, the growing nuclei experience a more uniform solution

concentration and spend similar residence time in the microchannel (Figure 1b). Therefore, synthesis in a hydrodynamically-focused stream generates a more homogenous particle size distribution owing to the uniformity of the fluid velocity, and thus reaction conditions.

HF devices can be divided into two categories: coaxial tube devices and on-chip planar devices. In an ideal flow focusing device, the central flow should be compressed both horizontally and vertically in order to obtain uniform fluid velocity both in horizontal and vertical planes which is also called three-dimensional (3D) focusing. Because of their simple fabrication and easy integration, on-chip based devices have been widely used in materials synthesis. However, due to the planar characteristics of most of the on-chip devices, two-dimensional (2D) HF focusing is more commonly utilized in those systems. Several microfluidic HF designs are reviewed in the following sections.

2.1 Coaxial tube microreactors

The simplest type of coaxial tube reactor is an assembly of two concentric capillary tubes connected to a channel in which a central flow is injected through the inner capillary tube, while the sheath flow is injected from the outer layer (Figure 2a) [38,39]. The central flow can be a mixture of chemical reagents, and the sheath flow can be either an immiscible or inactive fluid. The focal size (the diameter of the central flow) and the flow pattern (the shape of the central flow) can be finely tuned through the tube geometry, flow rates, flow rate ratio (FRR, the ratio of the sheath flow rate to the central flow rate), and the physical properties of the fluids. In co-axial flow focusing and droplet generation devices there is a transition from dripping to jetting defined by the Rayleigh–Plateau instability [40,41]. As the flow rate of the outer sheath flow increases, the diameter of the inner sample fluid decreases forming a jetting flow [41]. At very high flow rates, turbulences can occur in the flow patterns [42]. The capillary tubes may be made of silica, steel, or polymers. The flexibility of the choice of materials enables high temperature and pressure conditions. Other variations of these systems include merging pulled glass pipettes with PDMS molding technology to enable the integration of other on-chip components (Figure 2b) [43]. However, this process requires multiple fabrication steps, as well as precise alignment and assembly of these hybrid systems.

Coaxial tube microreactors have been used to synthesize various types and structures of NPs including monodispersed spherical titanium particles [38], iron oxide NPs [44], goethite nanoparticles [45], and fluorescent core/shell γ-Fe_2O_3@SiO_2 nanoparticles [46]. The size of the synthesized iron oxide NPs can be less than 7 nm depending on the device geometry and flow parameters. Moreover, the tunability of this technique is demonstrated by the result that the size of the titanium particles can be finely tuned from 40 to 150 nm by changing the diameter of the inner tube. Nevertheless, controlling only the flow rates as single parameter for tuning the synthesized product properties is more desirable since a single device can be used for multiple batches resulting in desired NP size distributions.

2.2 On-chip 2D HF devices

Chip-based flow synthesis techniques have become very attractive because they can be reproduced massively at low cost. Replica-molding and soft-lithography are the most

common fabrication methods for chip reactors. Fabrication of complex microchannel geometries does not require added complexity owing to the simplicity of the lithography process. Furthermore, the integration of different on-chip components, including microheaters, optical and electrochemical sensors can help to enable additional on-chip functions [47].

In on-chip HF devices, the focusing is typically bidimensional (2D), where the central flow is only focused in the horizontal plane [48]. The simplest design is comprised of a central flow that is squeezed by two sheath flows from two sides (Figure 3a) [49]. Using this geometry, the mixing time can be reduced to less than 50 microseconds [50]. In another design, the sheath-flow channel was tilted to a different angle than 90°, and additional sheath flow channels were added to avoid vortex formation, and to achieve more stable flow profiles (Figure 3b and 3c) [51–53]. To concentrate the final synthesis products, sheath flow can be separated from the synthesized products by using bifurcation in the outlets (Figure 3d) [54]. For multi-step synthesis processes in which certain dwelling time is required for each step, multiple HF steps can be added with an offset (Figure 3e) [55].

2.3 On chip 3D HF devices

3D HF focusing requires both horizontal and vertical focusing of the sample flows which can further improve the size uniformity of the synthesized nanomaterials. However, considering the planar property of the chip-based microfluidic devices, it is more difficult to achieve on-chip 3D HF than 2D HF. One straightforward way is to design multiple layer on-chip devices which can introduce sheath flow from top and bottom of the central flow, as well as the left and right at the same time, to squeeze the central flow in both horizontal and vertical direction [56]. Later, efforts were made to reduce the number of layers in order to decrease the required fabrication steps and cost. For example, by introducing a height variation in microfluidic channels using two-layer fabrication, focusing on the horizontal and vertical planes can be introduced sequentially to achieve 3D HF (Figure 4a and 4b) [30,57,58].

Single planar on-chip devices for 3D HF have been developed in an attempt to simplify device fabrication. Rhee *et al.* used a PDMS device with precisely aligned 3 vertical inlets and two horizontal side inlets to achieve 3D HF in single-layer microchannels, and synthesized size-tunable polymeric nanoparticles with smaller sizes and improved monodispersity compared to 2D HF or bulk synthesis method [59]. Even though these devices are single layer and provide 3D HF, extreme precision in device preparation and assembly is required. A more recent approach to 3D HF has been demonstrated using single layer planar devices with sequential PDMS posts [60,61]. However, these devices are used to sculpt the sample flow using inertial effects in order to fabricate shaped-defined polymeric 3D structures rather than synthesize NPs via spatiotemporal control of diffusion.

A more user-friendly, single-layer approach has been introduced by Mao *et al.* which employs a novel fluid manipulation technique called “microfluidic drifting” to generate 3D HF (Figure 5a) [62,63]. “Microfluidic drifting” refers to the lateral drift of the central flow, caused by the transverse secondary flow induced by the centrifugal effect in the curve of a microfluidic channel. The secondary flow is characterized by a pair of counter-rotating

vortices (Dean vortices) positioned in the upper and lower portion of the channel cross-sectional plane. This method is effective, robust and does not require any extensive fabrication techniques other than standard soft lithography. By using the counter-rotating vortices, a different design with contraction-expansion array (CEA) was implemented to achieve 3D HF with a single sheath flow in a single-layer planar device (Figure 5b) [64]. Kim *et al.* used the vertical asymmetry of the flow patterns arising from the parabolic velocity profile and micro vortex formation close to inlets in order to achieve 3D HF with a single-layer planar on-chip microfluidic device [65].

3. Scale-up for mass production

Even though microfluidic HF devices can often synthesize nanomaterials superior to those derived from bulk synthesis, the associated throughput is generally much lower compared to batch processes. This is an inherent property of microfluidic systems because they are designed to handle minute amount of fluids in laminar flow regime which provides high uniformity and precise control of chemical compositions. In doing so, a typical microfluidic HF reactor can only synthesize NPs in tens of milligrams per hour. For emerging new applications, such as synthesis of personalized medicine, which only requires small amount of products, the slow production rate of current microfluidic HF reactors can be sufficient. However, considering the ever-growing potential of NPs in industrial applications, and to realize the translation of microfluidic devices for more general biomedical and pharmaceutical applications, it is important to scale-up the synthesis process while maintaining the advantages of microfluidics in order to achieve mass production [66,67].

A simple approach to increase the throughput of microfluidic synthesis is to fabricate multiple identical on-chip HF devices working in parallel. However, in such an arrangement, each device needs a separate set of pumps or pressure controlling system for fluid supply. Thus, integration between these parallel on-chip devices is necessary to reduce the number of pumps and other peripheral equipment, and to maintain identical conditions in each device during the operation. Nisisako *et al.* used multi-array microfluidic modules to scale up production of emulsions and microbubbles (Figure 6), where they used radial array of junctions to produce compound droplets with a total flow rate as high as 120 mL/hour [68,69]. Kendall *et al.* developed a radial array of flow focusing droplet generators (FFDGs) to generate microbubbles for ultrasound imaging and drug delivery applications [70]. A similar study, using the same platform, demonstrated generation of more than 1 billion droplets per hour with an average diameter of 9.8 microns [71]. These devices can be easily implemented for on-chip 2D HF arrays by using two miscible liquids as the central and sheath flow for synthesizing NPs. In a recent study, Liu *et al.* utilized a coaxial glass reactor and controlled micromixing to achieve polymeric NP synthesis of about 240 grams per day [72]. Similar approaches have also been tried for increasing throughput of other diverse microfluidic synthesis devices with promising results [16,73–78], which shows potential for commercialization and adaptation of microfluidic HF based devices. Noting that, there is still room for improvement in terms of device simplicity and dexterity that can aid in mass production and applicability for different size NPs. In general, using very high flow rates in coaxial tube reactors that are made of hard materials is a simple solution to increase throughput. However; for reactions that requires certain dwell time for nuclei to reach a

desired NP size [45,79], this approach cannot be applied. In that case, for better tunability of NP size, parallelized reactions via connected inlets would be preferred.

4. Products of Microfluidic HF based Synthesis

4.1 Organic nanomaterials

Organic nanoparticles, such as polymer and lipid based NPs, often loaded with drugs, nucleic acids, or imaging components, are an important group of synthesized products that have great potential in the field of pharmaceutics and nanomedicine. The reduction in size to the nanoscale renders these particles bioavailable and targetable to specific tissues in biological systems. Polymer micro- and nanoparticles (NPs) are synthesized using photo-polymerization, precipitation, and crystallization, and can be used as targeted drug carriers. The fast mixing capability provided by microfluidic HF methods enables fine control of nucleation and growth processes which yields a narrow particle size distribution (Figure 7) [37]. Some examples of the organic NP products synthesized by HF are listed in Table 1. Thiele *et al.* used a PDMS based HF device to synthesize polymer NPs by focusing ethanolic block copolymer solution with two sheath flows of water [80]. By adjusting the sheath flow rates, ethanol concentration in the polymer solution was reduced and nucleation of NPs started. They observed an increase of particle size with decreasing flow rates, and vice versa. Karnik *et al.* studied the mechanism of the production of poly(lactic-co-glycolic acid)-b-poly-(ethylene glycol) (PLGA-PEG) block copolymer NPs in an on-chip 2D HF device (Figure 8) [37]. The solution of the polymer dissolved in acetonitrile was focused by water as the sheath flow. It was reported that as the flow rate ratio of the sheath flow to central flow increased, the width of the central flow decreased, and the size of NPs decreased. Based on their results, the authors hypothesized that NPs size was affected by the rate of mixing, which can be controlled by the flow rate ratio (Figure 9a and 9b) [81]. In a later study, they demonstrated that on-chip 3D HF yields a narrower NP size distribution compared to 2D focusing [59]. The reason is that 3D HF can provide a more homogenous flow profile and concentration uniformity in both horizontal and vertical planes, and prevent NP deposition to the channel walls which could eventually result in device clogging.

Liposomes are highly functional products of microfluidic HF method due to their ability to encapsulate aqueous components for delivery of genes, drugs and other therapeutic agents, and be used as contrast agents [82]. On-chip HF methods have the capacity to provide reduced polydispersity compared to batch processes which is essential in liposome based bio-applications [83–86]. Jahn *et al.* synthesized liposomes with mean sizes ranged from 50 nm to 150 nm using various flow rates of isopropylalcohol (IPA) lipid solution and two sheath flows of a buffer solution (Figure 10) [87]. Later, they demonstrated controllable drug loading into the synthesized liposomes in continuous flow mode [51,54]. Kennedy *et al.* used a 3D HF device in order to synthesize liposomes in the size range of 100–300 nm by changing sheath-to-core flow ratio, and concentrations of lipids and salts in the core and sheath flows, respectively [88]. The further study by Phapal *et al.* showed that, in 3D HF devices, the size distribution of liposomes is strongly affected in the convective mixing regime at high Peclet number ($Pe \gg 1$) [89]. Wi *et al.* utilized an on-chip 2D HF device with separation capability to synthesize and separate liposomes based on their size [90]. They

demonstrated that the size distribution of the liposomes depends on both flow rate ratio and synthesis temperature such that the liposomes synthesized at higher temperature (60 C) showed smaller mean sizes compared with liposomes synthesized at room temperature (25 C). This effect was caused by the reduced interfacial tension between the central lipid stream and the buffer sheath stream at high temperature, and enhanced mass transfer between the two streams. Lipid-polymer hybrid (LPH) nanoparticles have been synthesized in a single-layer 3D HF device with a high throughput of ~3 g/hour. It was also demonstrated that the particle size could be controlled (30–170 nm) by varying the flow rate (Reynolds number ranging from 30–150) and the polydispersity of the particles was relatively low (~0.1) [91].

The synthesis process of electrostatic complexation of DNA depends on many factors, such as buffer ionic strength, order of reagent addition, and type of reagents. Microfluidic HF enables better control over the diffusion/mixing process, and can be used to synthesize DNA complexes with desired sizes and narrow size distribution. Koh *et al.* synthesized Polyethylenimine (PEI) and plasmid DNA (pDNA) complexes using microfluidic 2D HF method with superior size uniformity and lower cytotoxicity compared to bulk synthesis [92]. Li et al. implemented a drifting flow based 3D HF method along with low-power acoustic exposure to synthesize polyplex (DNA/polymer) complexes with smaller size, higher transfection efficiency and lower cytotoxicity compared to bulk methods (Figure 11) [31].

4.2 Organic fibers

Hydrogel-based microfibers are interesting since they can be used to create tissue scaffolds for tissue engineering [93–95]. Conventionally, electrospinning method is often used for fiber fabrication. However, bulk electrospinning method lacks versatility in terms of adding desired functionality into the synthesized fibers. Adaptation of microfluidic HF technique enables fabrication of more functional and complex fibers with desired physical and compositional asymmetries [96–99]. Some examples of the organic fibers synthesized by HF are listed in Table 2. Coaxial tube HF devices have been widely used as a simple, cost effective and flexible method for microfiber fabrication. For example, Jeong *et al.* synthesized microfiber and tubes by using in-situ polymerization in an “on the fly” 3D HF device [43]. More complex Janus polyurethane microfibers have been synthesized using multiphase laminar flows and asymmetrically generated bubbles in order to create selective porosity for easy cell attachment [100,101]. The porosity of microfibers is an important parameter as it also affects the delivery of nutrients and oxygen. By using the immersion precipitation and solvent evaporation method, porous microfibers of amphiphilic triblock copolymer, poly(p-dioxanone-co-caprolactone-block-poly(ethylene oxide)-block-poly(p-dioxanone-co-caprolactone) (PPDO-co-PCL-b-PEG-b-PPDO-co-PCL) were synthesized [102]. Porous microfibers can be used to encapsulate drugs and proteins for better controlled release rate by tuning the degree of porosity. Using multiple laminar flows in multibarrel coaxial HF devices, Cheng *et al.* fabricated cell laden alginate microfibers for applications in 3D bio-architectures [103]. These pre-seeded microfibers can be potentially used in guided cell growth for damaged muscle and nerve repair. Onoe *et al.* synthesized hydrogel microfibers with encapsulated proteins and various differentiated cells using a coaxial HF device (Figure 12) [104]. Their fabrication yielded fascinating meter long cell-laden

microfibers that mimic physiological composition of various in vivo biological structures which can be used in some therapeutic applications including endoscopic surgery and catheter intervention.

4.3 Inorganic nanomaterials

Inorganic nanomaterials including metal and oxide NPs, and quantum dots (QDs) acquire unique chemical and physical properties, which can be very different from their bulk properties [105]. During a basic NP synthesis process, inorganic nanoparticles undergo self-assembly processes including nucleation, growth and agglomeration during their formation from solutions. The factors that determine their size include precursor concentration, reaction temperature, surfactant properties, and nuclei residence time. When the nanoparticles grow to the desired size and shape, the reaction is quenched by dispersing the nanoparticles into a buffer solution. Therefore, in order to synthesize homogeneous nanoparticles, it is important to induce rapid nucleation followed by controllable growth. Microfluidic HF methods enable the rapid nucleation by precise control of mixing time, reaction temperature and residence time, and therefore can produce inorganic nanoparticles with better size homogeneity compared to bulk synthesis. Some examples of the inorganic NP products synthesized by HF are listed in Table 3. In microfluidic HF devices, the size and the morphology of synthesized nanomaterials can be tuned by adjusting flow rates. For example, Puigmartí-Luis *et al.* demonstrated synthesis of quasi-1D, 1D and hallow nanowires, and 3D microcrystals within the same device, while only changing the flow rates, using the fact that the mixing of compounds by diffusion strongly depends on the flow conditions [106].

Noble metal nanomaterials including gold and silver NPs are interesting because of their potential in biomedical applications [107]. The size and shape of metal NPs affect their physical properties and biological functions. For example, the extinction spectra of gold and silver nanoparticles, and the uptake of gold nanoparticles by mammalian cells, depend on their size and shape [108]. Metal nanoparticle synthesis is performed generally by reducing the metal ion precursor with application of stabilizing ligands. For this type of synthesis, a two-phase or droplet based microfluidic device is used more often. Lazarus *et al.* synthesized monodispersed gold nanoparticles using ionic liquids in an on-chip device [36,109]. A stream of pure 1-butyl-3-methylimidazolium tetrafluoroborate (BMIM-BF_4) was injected with two side-flow of reagents ($HAuCl_4$/l-methyl-imidazole and $NaBH_4$ in BMIM-BF_4), and later focused by an inert polychlorotrifluoroethylene oil. Based on the flow rates, the stream of the reagent can be continuous or broken into single droplets. The synthesized particles showed larger mean size (5.65 ± 1.03 nm) and increased polydispersity (CV: 18.2%) in the case of continuous flow. While by droplet formation, the particles became smaller (4.38 ± 0.53 nm) and more homogeneous (CV: 12.1%). Microdroplet-based synthesis take advantage of the small volume (nano or pico liter) and the counter-rotating recirculation within droplets to reach fast mixing and homogeneous fluid environment, resulting in good uniformity of products making it attractive in nanomaterials synthesis. However, droplet based synthesis requires involvement of two-phase fluids and surfactants, adding purification as an additional step after the completion of the synthesis. For certain type of applications which are sensitive to even small traces of contaminations, such as

gene-based therapy, HF based synthesis shows advantage over droplet-based synthesis in reducing number of steps and avoiding contamination.

Metal oxide nanoparticles, especially iron oxide NPs, have a wide range of functions in biomedical applications including contrast agents for Magnetic Resonance Imaging, targeted drug delivery, and magnetic hyperthermia for therapeutic treatments [110]. Iron oxide (Fe_3O_4 or γ-Fe_2O_3) and goethite nanoparticles (α-FeOOH) have been synthesized in microfluidic coaxial tube reactors by injecting an aqueous solution of iron chloride as the central flow, and a basic solution of NaOH, NH_4OH or tetramethylammonium hydroxide (TMAOH) as the sheath flow [45,111,112]. The nucleation and growth occurs at the interface of two flows, which is separated from the channel walls. Homogeneous nanoparticles were synthesized without sticking on the channel wall. Because the synthesis of Fe_3O_4 nanoparticles involves a rapid change in pH to avoid the formation of FeOOH, it is important to monitor the pH distribution in the channel. The pH profile in this device was validated by using fluorescence confocal laser scanning microscopy, demonstrating that the HF technique enables a well-defined pH variation within the streams [112]. Fluorescent silica-coated magnetic nanoparticles have also been prepared in a multistep coaxial tube system [46]. In this NP design, the γ-Fe_2O_3 NPs enable targeting via their magnetic property, and the silica shells protect the inner NP and enable optical labelling by incorporation of chromophores. These particles can be used as contrast agents for molecular imaging. Besides biomedical applications, inorganic NPs have been synthesized for solar cells, light emitting diodes (LEDs), gas sensors, and heterogeneous catalysts [113]. For example, Roig *et al.* used coaxial tube devices and synthesized UV-emitting ZnO nanoparticles with pure excitonic photoluminescence for application in UV-LEDs [114].

The above discussed products including many others such as quantum dots (QD) [115] and inorganic and organic hybrid nanomaterials [32,116–119] reveal the immense potential and applicability of the on-chip HF methods for synthesizing nano/biomaterials with precise concentration, size and chemical properties.

5. Microfluidic HF devices for Study of Reaction Mechanics

In addition to the synthesis of nanomaterials, microfluidic HF methods can be used as a tool to study the synthetic processes or chemical reaction kinetics. Conventionally, the study of reaction kinetics is performed in stopped-flow devices, while the reaction is triggered by a turbulent mixer. In this mode of operation, no meaningful measurement can be performed before completing the mixing, and this time period is call “dead time”. In conventional stopped-flow devices, the “dead time” is typically ~ 1 ms, and the volume is typically ~ 1 mL per test [120]. Microfluidic HF technique can reduce the “dead time” (~ 1 to 10 μs) by squeezing the central sample flow to a very narrow stream [121]. This reduced “dead time” is small compare to the time required for most of the reactions to take place, and therefore we can consider that the reaction starts at the same time and continuously progresses in the focused stream. The extremely small sample flow allows significantly reduced sample consumption compared to bulk methods, which is essentially important for experiments involving expensive biomaterials or scarce samples. The confinement of the sample flow also enables epifluorescence based optical monitoring without the need of confocal

microscopy. Furthermore, since the sample flow is focused to a narrow stream in the center of the microchannel, its velocity distribution is nearly uniform, making it possible to convert the reaction time to positional coordinates with the already known velocity information. Once the change of fluorescence signal is detected at a certain position in the channel, we can convert it back to get the reaction time by dividing the distance by the velocity. Therefore, unlike conventional methods, which have to perform the measurement in real time, the measurement in microfluidic HF device can be done at any time. Thanks to the high resolution imaging capabilities, it is also easy to obtain accurate time information within microfluidic HF devices. For example, Gambin *et al.* proposed an on-chip 3D HF device to study kinetics of biochemical reactions, such as folding of proteins and RNA using fluorescence image velocimetry technique [122]. They used the velocity and special position data of the fluorescent dye to obtain very precise measurement of the reaction time.

Unlike batch processing methods, in which the product is the result of various reaction conditions (shear rate, chemical concentration, temperature, etc.), since the reaction condition within the focused sample flow is nearly uniform, products synthesized with HF are often more homogeneous after forming under well-defined reaction conditions. Therefore, for synthetic processes that cannot be easily visualized, product disposition can be followed with the change of reaction conditions in microfluidic HF devices. During the synthesis of liposomes using a microfluidic HF device, Jahn *et al.* found that the size of the liposomes was weakly affected by the lipid concentration, or the flow rates while keeping the ratio between the sheath flow and central flow as constant [51]. However, the liposome size strongly depends on flow rate ratio (FRR) between the sheath and central flow. Based on the experimental result, they hypothesized that higher solvent content can potentially stabilize the bilayer phospholipid fragment (BPF) and allow larger congregation of lipids to yield larger BPFs. When the FRR is small, the central stream (lipid solvent) is wider, and the mixing time required for the solvent to diffuse out into the water phase is elongated. During this process, larger vesicles with broader distribution are formed. In contrast, when the FRR is large, the central stream is narrow, and the time required for the solvent to diffuse into the water phase is short. This quick diffusion limits the formation of big BPFs, resulting in smaller liposomes with high homogeneity. Currently there is no technique that can be used to directly visualize the liposome formation due to the high flow velocity in microfluidic channel, but the HF method provides a way to study the liposome synthesis process. Jiang *et al.* synthesized aromatic organic nanoparticles in an on-chip 3D HF device [81]. By studying the dynamics of solvent depletion in the focused stream by finite element computation method, they found the size and size distribution of the self-assembled aromatic nanoparticles strongly depend on the speed of solvent depletion. Thanks to the fast depletion enabled by the 3D HF device, aromatic nanoparticles with a narrow size distribution could be synthesized.

6. Perspective

Microfluidic HF has proved itself as an economical, simple and powerful tool for the synthesis of nanomaterials with high monodispersity and reproducibility. On-chip HF devices have become popular due to their low cost, flexibility and ease of monitoring. 3D HF devices offer superior focusing performance compared to 2D HF devices by providing a

highly uniform velocity profile and rapid mixing in the focused stream. Noting that, the on-chip 3D HF devices are still at their early stage due to the challenge of multi-layer fabrication and competition with other focusing mechanisms and device designs. A new approach for fabricating more intricate devices is to embrace 3D printing technologies that enable scale-up production. Various new features can be easily integrated into an HF device to achieve a higher degree of complexity and increased functionality.

Besides nanomaterials synthesis, HF devices are powerful tools to study the reaction kinetics and synthesis mechanisms by translating spatial data into temporal information. There are tremendous opportunities to apply this tool for studying fast reactions such as protein or RNA folding. Furthermore, combining the advantages of HF devices with other on-chip sensors (on-chip plasmonic sensor, SERS sensor, nanowire resistant sensor, etc.) can further improve the sensitivity and accuracy of these kinetic studies. All these capabilities can be used to explore new chemical reactions and molecular pathways in a simple and economical device.

Two research directions likely to advance HF-based technologies are miniaturization and fluid handling technologies. First, it is important to miniaturize the whole system including the pump/pressure tank to enable on-site synthesis, which will be useful for the synthesis of nanomedicines, particularly those that are radioactive, with a very short shelf life. As the field of “organ-on-chip” matures, it may be possible to integrate nanomedicine synthesis with fast screening to benefit personalized medicine applications. Second, for on-chip HF-based synthesis, adaptation of chip-based fluid handling technologies should be considered as alternatives to bulky external pumps. For example, simpler chip-based pumps [123] in HF devices could facilitate synchronized parallel reactions and system integration, two aspects crucial for HF device commercialization.

To push the translation of HF devices from the realm of basic research to industrial and clinical applications, challenges remain as to fully integrating the processes of synthesis, monitoring, and device scale-up for mass production. It is also important to note that, additional purification mechanisms should be developed to remove the synthesized products and organic solvents similar to the industrial level purification processes [124,125]. It may be possible to optimize the throughput with massively parallel channels [85], akin to how massively parallel computer processing can significantly enhance the capability of computational networks. When that happens, HF-based synthesis will have a significant impact on the nanomaterials field.

Acknowledgments

Support from NIH (AI096305, HL109442, GM110494, GM112048, EB019785), NSF (IDBR-1455658), and W81XWH-12-1-0261 is acknowledged.

References

1. Qasaimeh MA, Ricoult SG, Juncker D. Microfluidic probes for use in life sciences and medicine. Lab Chip. 2013; 13:40–50. DOI: 10.1039/C2LC40898H [PubMed: 23042577]
2. Lin W-Y, Wang Y, Wang S, Tseng H-R. Integrated microfluidic reactors. Nano Today. 2009; 4:470–481. DOI: 10.1016/j.nantod.2009.10.007 [PubMed: 20209065]

3. Velve-Casquillas G, Le Berre M, Piel M, Tran PT. Microfluidic tools for cell biological research. Nano Today. 2010; 5:28–47. DOI: 10.1016/j.nantod.2009.12.001 [PubMed: 21152269]
4. Gaharwar AK, Detamore MS, Khademhosseini A. Emerging Trends in Biomaterials Research. Ann Biomed Eng. 2016; 44:1861–1862. DOI: 10.1007/s10439-016-1644-0 [PubMed: 27184493]
5. Zhang Y, Park S, Yang S, Wang T-H. An all-in-one microfluidic device for parallel DNA extraction and gene analysis. Biomed Microdevices. 2010; 12:1043–1049. DOI: 10.1007/s10544-010-9458-6 [PubMed: 20632111]
6. Zhang J, Yan S, Yuan D, Alici G, Nguyen N-T, Ebrahimi Warkiani M, Li W. Fundamentals and applications of inertial microfluidics: a review. Lab Chip. 2016; 16:10–34. DOI: 10.1039/C5LC01159K [PubMed: 26584257]
7. Kovarik ML, Gach PC, Ornoff DM, Wang Y, Balowski J, Farrag L, Allbritton NL. Micro Total Analysis Systems for Cell Biology and Biochemical Assays. Anal Chem. 2012; 84:516–540. DOI: 10.1021/ac202611x [PubMed: 21967743]
8. Elvira KS, Solvas XCi, Wootton RCR, DeMello AJ. The past, present and potential for microfluidic reactor technology in chemical synthesis. Nat Chem. 2013; 5:905–915. DOI: 10.1038/nchem.1753 [PubMed: 24153367]
9. Khan IU, Serra CA, Anton N, Vandamme TF. Production of nanoparticle drug delivery systems with microfluidics tools. Expert Opin Drug Deliv. 2015; 12:547–562. DOI: 10.1517/17425247.2015.974547 [PubMed: 25345543]
10. Seo M, Nie Z, Xu S, Mok M, Lewis PC, Graham R, Kumacheva E. Continuous Microfluidic Reactors for Polymer Particles. Langmuir. 2005; 21:11614–11622. DOI: 10.1021/la050519e [PubMed: 16316091]
11. Il Park J, Saffari A, Kumar S, Günther A, Kumacheva E. Microfluidic Synthesis of Polymer and Inorganic Particulate Materials. Annu Rev Mater Res. 2010; 40:415–443. DOI: 10.1146/annurev-matsci-070909-104514
12. Zhang L, Wang Y, Tong L, Xia Y. Synthesis of Colloidal Metal Nanocrystals in Droplet Reactors: The Pros and Cons of Interfacial Adsorption. Nano Lett. 2014; 14:4189–4194. DOI: 10.1021/nl501994q [PubMed: 24960241]
13. Duncanson WJ, Lin T, Abate AR, Seiffert S, Shah RK, Weitz DA. Microfluidic synthesis of advanced microparticles for encapsulation and controlled release. Lab Chip. 2012; 12:2135.doi: 10.1039/c2lc21164e [PubMed: 22510961]
14. Choi K, Ng AHC, Fobel R, Wheeler AR. Digital Microfluidics. Annu Rev Anal Chem. 2012; 5:413–440. DOI: 10.1146/annurev-anchem-062011-143028
15. Reynolds O. An Experimental Investigation of the Circumstances Which Determine Whether the Motion of Water Shall Be Direct or Sinuous, and of the Law of Resistance in Parallel Channels. Philos Trans R Soc London. 1883; 174:935–982. DOI: 10.1098/rstl.1883.0029
16. Lim J-M, Swami A, Gilson LM, Chopra S, Choi S, Wu J, Langer R, Karnik R, Farokhzad OC. Ultra-High Throughput Synthesis of Nanoparticles with Homogeneous Size Distribution Using a Coaxial Turbulent Jet Mixer. ACS Nano. 2014; 8:6056–6065. DOI: 10.1021/nn501371n [PubMed: 24824296]
17. Lee C-Y, Chang C-L, Wang Y-N, Fu L-M. Microfluidic Mixing: A Review. Int J Mol Sci. 2011; 12:3263–3287. DOI: 10.3390/ijms12053263 [PubMed: 21686184]
18. Lu Liang-HsuanRyu Kee SukLiu Chang. A magnetic microstirrer and array for microfluidic mixing. J Microelectromechanical Syst. 2002; 11:462–469. DOI: 10.1109/JMEMS.2002.802899
19. Zhu G-P, Nguyen N-T. Rapid magnetofluidic mixing in a uniform magnetic field. Lab Chip. 2012; 12:4772.doi: 10.1039/c2lc40818j [PubMed: 22990170]
20. Chang C-C, Yang R-J. Electrokinetic mixing in microfluidic systems. Microfluid Nanofluidics. 2007; 3:501–525. DOI: 10.1007/s10404-007-0178-z
21. Ahmed D, Peng X, Ozcelik A, Zheng Y, Huang TJ. Acousto-plasmofluidics: Acoustic modulation of surface plasmon resonance in microfluidic systems. AIP Adv. 2015; 5:97161.doi: 10.1063/1.4931641
22. Ozcelik A, Ahmed D, Xie Y, Nama N, Qu Z, Nawaz AA, Huang TJ. An Acoustofluidic Micromixer via Bubble Inception and Cavitation from Microchannel Sidewalls. Anal Chem. 2014; 86:5083–5088. DOI: 10.1021/ac5007798 [PubMed: 24754496]

23. Ahmed D, Muddana HS, Lu M, French JB, Ozcelik A, Fang Y, Butler PJ, Benkovic SJ, Manz A, Huang TJ. Acoustofluidic Chemical Waveform Generator and Switch. Anal Chem. 2014; 86:11803–11810. DOI: 10.1021/ac5033676 [PubMed: 25405550]
24. Hellman AN, Rau KR, Yoon HH, Bae S, Palmer JF, Phillips KS, Allbritton NL, Venugopalan V. Laser-Induced Mixing in Microfluidic Channels. Anal Chem. 2007; 79:4484–4492. DOI: 10.1021/ac070081i [PubMed: 17508715]
25. Yang A-S, Chuang F-C, Chen C-K, Lee M-H, Chen S-W, Su T-L, Yang Y-C. A high-performance micromixer using three-dimensional Tesla structures for bio-applications. Chem Eng J. 2015; 263:444–451. DOI: 10.1016/j.cej.2014.11.034
26. Hossain S, Ansari MA, Husain A, Kim K-Y. Analysis and optimization of a micromixer with a modified Tesla structure. Chem Eng J. 2010; 158:305–314. DOI: 10.1016/j.cej.2010.02.002
27. Kang TG, Singh MK, Anderson PD, Meijer HEH. A chaotic serpentine mixer efficient in the creeping flow regime: from design concept to optimization. Microfluid Nanofluidics. 2009; 7:783–794. DOI: 10.1007/s10404-009-0437-2
28. Buchegger W, Wagner C, Lendl B, Kraft M, Vellekoop MJ. A highly uniform lamination micromixer with wedge shaped inlet channels for time resolved infrared spectroscopy. Microfluid Nanofluidics. 2011; 10:889–897. DOI: 10.1007/s10404-010-0722-0
29. Simonnet C, Groisman A. Two-dimensional hydrodynamic focusing in a simple microfluidic device. Appl Phys Lett. 2005; 87:114104.doi: 10.1063/1.2046729
30. Chiu Y-J, Cho SH, Mei Z, Lien V, Wu T-F, Lo Y-H. Universally applicable three-dimensional hydrodynamic microfluidic flow focusing. Lab Chip. 2013; 13:1803.doi: 10.1039/c3lc41202d [PubMed: 23493956]
31. Lu M, Ho Y-P, Grigsby CL, Nawaz AA, Leong KW, Huang TJ. Three-Dimensional Hydrodynamic Focusing Method for Polyplex Synthesis. ACS Nano. 2014; 8:332–339. DOI: 10.1021/nn404193e [PubMed: 24341632]
32. Lu M, Yang S, Ho Y-P, Grigsby CL, Leong KW, Huang TJ. Shape-Controlled Synthesis of Hybrid Nanomaterials via Three-Dimensional Hydrodynamic Focusing. ACS Nano. 2014; 8:10026–10034. DOI: 10.1021/nn502549v [PubMed: 25268035]
33. Zhigaltsev IV, Belliveau N, Hafez I, Leung AKK, Huft J, Hansen C, Cullis PR. Bottom-Up Design and Synthesis of Limit Size Lipid Nanoparticle Systems with Aqueous and Triglyceride Cores Using Millisecond Microfluidic Mixing. Langmuir. 2012; 28:3633–3640. DOI: 10.1021/la204833h [PubMed: 22268499]
34. Sinha B, Müller RH, Möschwitzer JP. Bottom-up approaches for preparing drug nanocrystals: Formulations and factors affecting particle size. Int J Pharm. 2013; 453:126–141. DOI: 10.1016/j.ijpharm.2013.01.019 [PubMed: 23333709]
35. Liberman A, Mendez N, Trogler WC, Kummel AC. Synthesis and surface functionalization of silica nanoparticles for nanomedicine. Surf Sci Rep. 2014; 69:132–158. DOI: 10.1016/j.surfrep.2014.07.001 [PubMed: 25364083]
36. Lazarus LL, Yang ASJ, Chu S, Brutchey RL, Malmstadt N. Flow-focused synthesis of monodisperse gold nanoparticles using ionic liquids on a microfluidic platform. Lab Chip. 2010; 10:3377.doi: 10.1039/c0lc00297f [PubMed: 21057686]
37. Karnik R, Gu F, Basto P, Cannizzaro C, Dean L, Kyei-Manu W, Langer R, Farokhzad OC. Microfluidic Platform for Controlled Synthesis of Polymeric Nanoparticles. Nano Lett. 2008; 8:2906–2912. DOI: 10.1021/nl801736q [PubMed: 18656990]
38. Takagi M, Maki T, Miyahara M, Mae K. Production of titania nanoparticles by using a new microreactor assembled with same axle dual pipe. Chem Eng J. 2004; 101:269–276. DOI: 10.1016/j.cej.2003.11.011
39. Pabit SaHagen SJ. Laminar-Flow Fluid Mixer for Fast Fluorescence Kinetics Studies. Biophys J. 2002; 83:2872–2878. DOI: 10.1016/S0006-3495(02)75296-X [PubMed: 12414719]
40. Utada AS, Chu L-Y, Fernandez-Nieves A, Link DR, Holtze C, Weitz DA. Dripping, Jetting, Drops, and Wetting: The Magic of Microfluidics. MRS Bull. 2007; 32:702–708. DOI: 10.1557/mrs2007.145

41. Nunes JK, Tsai SSH, Wan J, Stone HA. Dripping and jetting in microfluidic multiphase flows applied to particle and fibre synthesis. J Phys D Appl Phys. 2013; 46:114002.doi: 10.1088/0022-3727/46/11/114002 [PubMed: 23626378]
42. Andreev VP, Koleshko SB, Holman DA, Scampavia LD, Christian GD. Hydrodynamics and Mass Transfer of the Coaxial Jet Mixer in Flow Injection Analysis. Anal Chem. 1999; 71:2199–2204. DOI: 10.1021/ac981037t [PubMed: 21662757]
43. Jeong W, Kim J, Kim S, Lee S, Mensing G, Beebe DJ. Hydrodynamic microfabrication via “on the fly” photopolymerization of microscale fibers and tubes. Lab Chip. 2004; 4:576–580. DOI: 10.1039/B411249K [PubMed: 15570368]
44. Salazar-Alvarez G, Muhammed M, Zagorodni AA. Novel flow injection synthesis of iron oxide nanoparticles with narrow size distribution. Chem Eng Sci. 2006; 61:4625–4633. DOI: 10.1016/j.ces.2006.02.032
45. Abou-Hassan A, Sandre O, Neveu S, Cabuil V. Synthesis of Goethite by Separation of the Nucleation and Growth Processes of Ferrihydrite Nanoparticles Using Microfluidics. Angew Chemie Int Ed. 2009; 48:2342–2345. DOI: 10.1002/anie.200805933
46. Abou-Hassan A, Bazzi R, Cabuil V. Multistep Continuous-Flow Microsynthesis of Magnetic and Fluorescent γ-Fe 2 O 3 @SiO 2 Core/Shell Nanoparticles. Angew Chemie Int Ed. 2009; 48:7180–7183. DOI: 10.1002/anie.200902181
47. Daniele MA, Boyd DA, Mott DR, Ligler FS. 3D hydrodynamic focusing microfluidics for emerging sensing technologies. Biosens Bioelectron. 2015; 67:25–34. DOI: 10.1016/j.bios.2014.07.002 [PubMed: 25041926]
48. Lee G-B, Chang C-C, Huang S-B, Yang R-J. The hydrodynamic focusing effect inside rectangular microchannels. J Micromechanics Microengineering. 2006; 16:1024–1032. DOI: 10.1088/0960-1317/16/5/020
49. Majedi FS, Hasani-Sadrabadi MM, Emami SH, Taghipoor M, Dashtimoghadam E, Bertsch A, Moaddel H, Renaud P. Microfluidic synthesis of chitosan-based nanoparticles for fuel cell applications. Chem Commun. 2012; 48:7744.doi: 10.1039/c2cc33253a
50. Knight JB, Vishwanath A, Brody JP, Austin RH. Hydrodynamic Focusing on a Silicon Chip: Mixing Nanoliters in Microseconds. Phys Rev Lett. 1998; 80:3863–3866. DOI: 10.1103/PhysRevLett.80.3863
51. Jahn A, Stavis SM, Hong JS, Vreeland WN, DeVoe DL, Gaitan M. Microfluidic Mixing and the Formation of Nanoscale Lipid Vesicles. ACS Nano. 2010; 4:2077–2087. DOI: 10.1021/nn901676x [PubMed: 20356060]
52. Lo CT, Jahn A, Locascio LE, Vreeland WN. Controlled Self-Assembly of Monodisperse Niosomes by Microfluidic Hydrodynamic Focusing. Langmuir. 2010; 26:8559–8566. DOI: 10.1021/la904616s [PubMed: 20146467]
53. Park HY, Qiu X, Rhoades E, Korlach J, Kwok LW, Zipfel WR, Webb WW, Pollack L. Achieving uniform mixing in a microfluidic device: hydrodynamic focusing prior to mixing. Anal Chem. 2006; 78:4465–73. DOI: 10.1021/ac060572n [PubMed: 16808455]
54. Jahn A, Vreeland WN, DeVoe DL, Locascio LE, Gaitan M. Microfluidic Directed Formation of Liposomes of Controlled Size. Langmuir. 2007; 23:6289–6293. DOI: 10.1021/la070051a [PubMed: 17451256]
55. Koh CG, Zhang X, Liu S, Golan S, Yu B, Yang X, Guan J, Jin Y, Talmon Y, Muthusamy N, Chan KK, Byrd JC, Lee RJ, Marcucci G, Lee LJ. Delivery of antisense oligodeoxyribonucleotide lipopolyplex nanoparticles assembled by microfluidic hydrodynamic focusing. J Control Release. 2010; 141:62–69. DOI: 10.1016/j.jconrel.2009.08.019 [PubMed: 19716852]
56. Sundararajan N, Pio MS, Lee LP, Berlin AA. Three-Dimensional Hydrodynamic Focusing in Polydimethylsiloxane (PDMS) Microchannels. J Microelectromechanical Syst. 2004; 13:559–567. DOI: 10.1109/JMEMS.2004.832196
57. Kennedy MJ, Stelick SJ, Sayam LG, Yen A, Erickson D, Batt CA. Hydrodynamic optical alignment for microflow cytometry. Lab Chip. 2011; 11:1138.doi: 10.1039/c0lc00500b [PubMed: 21279198]

58. Chang C-C, Huang Z-X, Yang R-J. Three-dimensional hydrodynamic focusing in two-layer polydimethylsiloxane (PDMS) microchannels. J Micromechanics Microengineering. 2007; 17:1479–1486. DOI: 10.1088/0960-1317/17/8/009
59. Rhee M, Valencia PM, Rodriguez MI, Langer R, Farokhzad OC, Karnik R. Synthesis of Size-Tunable Polymeric Nanoparticles Enabled by 3D Hydrodynamic Flow Focusing in Single-Layer Microchannels. Adv Mater. 2011; 23:H79–H83. DOI: 10.1002/adma.201004333 [PubMed: 21433105]
60. Paulsen KS, Di Carlo D, Chung AJ. Optofluidic fabrication for 3D-shaped particles. Nat Commun. 2015; 6:6976.doi: 10.1038/ncomms7976 [PubMed: 25904062]
61. Wu C-Y, Owsley K, Di Carlo D. Rapid Software-Based Design and Optical Transient Liquid Molding of Microparticles. Adv Mater. 2015; 27:7970–7978. DOI: 10.1002/adma.201503308 [PubMed: 26509252]
62. Mao X, Lin S-CS, Dong C, Huang TJ. Single-layer planar on-chip flow cytometer using microfluidic drifting based three-dimensional (3D) hydrodynamic focusing. Lab Chip. 2009; 9:1583.doi: 10.1039/b820138b [PubMed: 19458866]
63. Mao X, Waldeisen JR, Huang TJ. "Microfluidic drifting"—implementing three-dimensional hydrodynamic focusing with a single-layer planar microfluidic device. Lab Chip. 2007; 7:1260.doi: 10.1039/b711155j [PubMed: 17896008]
64. Lee MG, Choi S, Park J-K. Three-dimensional hydrodynamic focusing with a single sheath flow in a single-layer microfluidic device. Lab Chip. 2009; 9:3155.doi: 10.1039/b910712f [PubMed: 19823733]
65. Kim Y, Joshi SD, Davidson La, LeDuc PR, Messner WC. Dynamic control of 3D chemical profiles with a single 2D microfluidic platform. Lab Chip. 2011; 11:2182.doi: 10.1039/c1lc20077a [PubMed: 21528131]
66. Wang H, Liu K, Chen K-J, Lu Y, Wang S, Lin W-Y, Guo F, Kamei K, Chen Y-C, Ohashi M, Wang M, Garcia MA, Zhao X-Z, Shen CKF, Tseng H-R. A Rapid Pathway Toward a Superb Gene Delivery System: Programming Structural and Functional Diversity into a Supramolecular Nanoparticle Library. ACS Nano. 2010; 4:6235–6243. DOI: 10.1021/nn101908e [PubMed: 20925389]
67. Liu Y, Du J, Choi J, Chen K-J, Hou S, Yan M, Lin W-Y, Chen KS, Ro T, Lipshutz GS, Wu L, Shi L, Lu Y, Tseng H-R, Wang H. A High-Throughput Platform for Formulating and Screening Multifunctional Nanoparticles Capable of Simultaneous Delivery of Genes and Transcription Factors. Angew Chemie Int Ed. 2016; 55:169–173. DOI: 10.1002/anie.201507546
68. Nisisako T, Ando T, Hatsuzawa T. High-volume production of single and compound emulsions in a microfluidic parallelization arrangement coupled with coaxial annular world-to-chip interfaces. Lab Chip. 2012; 12:3426.doi: 10.1039/c2lc40245a [PubMed: 22806835]
69. Nisisako T, Torii T. Microfluidic large-scale integration on a chip for mass production of monodisperse droplets and particles. Lab Chip. 2008; 8:287–293. DOI: 10.1039/B713141K [PubMed: 18231668]
70. Kendall MR, Bardin D, Shih R, Dayton PA, Lee AP. Scaled-up production of monodisperse, dual layer microbubbles using multi-array microfluidic module for medical imaging and drug delivery. Bubble Sci Eng Technol. 2012; 4:12–20. DOI: 10.1179/1758897912Y.0000000004 [PubMed: 23049622]
71. Bardin D, Kendall MR, Dayton PA, Lee AP. Parallel generation of uniform fine droplets at hundreds of kilohertz in a flow-focusing module. Biomicrofluidics. 2013; 7:34112.doi: 10.1063/1.4811276 [PubMed: 24404032]
72. Liu D, Cito S, Zhang Y, Wang C-F, Sikanen TM, Santos HA. A Versatile and Robust Microfluidic Platform Toward High Throughput Synthesis of Homogeneous Nanoparticles with Tunable Properties. Adv Mater. 2015; 27:2298–2304. DOI: 10.1002/adma.201405408 [PubMed: 25684077]
73. Hood RR, DeVoe DL. High-Throughput Continuous Flow Production of Nanoscale Liposomes by Microfluidic Vertical Flow Focusing. Small. 2015; 11:5790–5799. DOI: 10.1002/smll.201501345 [PubMed: 26395346]

74. Lim J, Caen O, Vrignon J, Konrad M, Taly V, Baret J-C. Parallelized ultra-high throughput microfluidic emulsifier for multiplex kinetic assays. Biomicrofluidics. 2015; 9:34101.doi: 10.1063/1.4919415
75. Le Goff GC, Lee J, Gupta A, Hill WA, Doyle PS. High-Throughput Contact Flow Lithography. Adv Sci. 2015; 2:1500149.doi: 10.1002/advs.201500149
76. Femmer T, Jans A, Eswein R, Anwar N, Moeller M, Wessling M, Kuehne AJC. High-Throughput Generation of Emulsions and Microgels in Parallelized Microfluidic Drop-Makers Prepared by Rapid Prototyping. ACS Appl Mater Interfaces. 2015; 7:12635–12638. DOI: 10.1021/acsami.5b03969 [PubMed: 26040198]
77. Uson L, Sebastian V, Arruebo M, Santamaria J. Continuous microfluidic synthesis and functionalization of gold nanorods. Chem Eng J. 2016; 285:286–292. DOI: 10.1016/j.cej.2015.09.103
78. Min K-I, Im DJ, Lee H-J, Kim D-P. Three-dimensional flash flow microreactor for scale-up production of monodisperse PEG–PLGA nanoparticles. Lab Chip. 2014; 14:3987–3992. DOI: 10.1039/C4LC00700J [PubMed: 25133684]
79. Polte J, Erler R, Thünemann AF, Sokolov S, Ahner TT, Rademann K, Emmerling F, Kraehnert R. Nucleation and Growth of Gold Nanoparticles Studied via in situ Small Angle X-ray Scattering at Millisecond Time Resolution. ACS Nano. 2010; 4:1076–1082. DOI: 10.1021/nn901499c [PubMed: 20088602]
80. Thiele J, Steinhauser D, Pfohl T, Förster S. Preparation of Monodisperse Block Copolymer Vesicles via Flow Focusing in Microfluidics. Langmuir. 2010; 26:6860–6863. DOI: 10.1021/la904163v [PubMed: 20121049]
81. Jiang L, Wang W, Chau Y, Yao S. Controllable formation of aromatic nanoparticles in a three-dimensional hydrodynamic flow focusing microfluidic device. RSC Adv. 2013; 3:17762.doi: 10.1039/c3ra42071j
82. Pattni BS, Chupin VV, Torchilin VP. New Developments in Liposomal Drug Delivery. Chem Rev. 2015; 115:10938–10966. DOI: 10.1021/acs.chemrev.5b00046 [PubMed: 26010257]
83. Jahn A, Reiner JE, Vreeland WN, DeVoe DL, Locascio LE, Gaitan M. Preparation of nanoparticles by continuous-flow microfluidics. J Nanoparticle Res. 2008; 10:925–934. DOI: 10.1007/s11051-007-9340-5
84. Wang X, Huang X, Yang Z, Gallego-Perez D, Ma J, Zhao X, Xie J, Nakano I, Lee LJ. Targeted delivery of tumor suppressor microRNA-1 by transferrin-conjugated lipopolyplex nanoparticles to patient-derived glioblastoma stem cells. Curr Pharm Biotechnol. 2014; 15:839–46. http://www.ncbi.nlm.nih.gov/pubmed/25374033. [PubMed: 25374033]
85. Huang X, Caddell R, Yu B, Xu S, Theobald B, Lee LJ, Lee RJ. Ultrasound-enhanced microfluidic synthesis of liposomes. Anticancer Res. 2010; 30:463–6. doi:20332455. [PubMed: 20332455]
86. Wu Y, Li L, Mao Y, Lee LJ. Static micromixer-coaxial electrospray synthesis of theranostic lipoplexes. ACS Nano. 2012; 6:2245–52. DOI: 10.1021/nn204300s [PubMed: 22320282]
87. Jahn A, Vreeland WN, Gaitan M, Locascio LE. Controlled Vesicle Self-Assembly in Microfluidic Channels with Hydrodynamic Focusing. J Am Chem Soc. 2004; 126:2674–2675. DOI: 10.1021/ja0318030 [PubMed: 14995164]
88. Kennedy MJ, Ladouceur HD, Moeller T, Kirui D, Batt CA. Analysis of a laminar-flow diffusional mixer for directed self-assembly of liposomes. Biomicrofluidics. 2012; 6:44119.doi: 10.1063/1.4772602 [PubMed: 24348890]
89. Phapal SM, Sunthar P. Influence of micro-mixing on the size of liposomes self-assembled from miscible liquid phases. Chem Phys Lipids. 2013; 172–173:20–30. DOI: 10.1016/j.chemphyslip.2013.04.006
90. Wi R, Oh Y, Chae C, Kim DH. Formation of liposome by microfluidic flow focusing and its application in gene delivery. Korea-Australia Rheol J. 2012; 24:129–135. DOI: 10.1007/s13367-012-0015-0
91. Kim Y, Lee Chung B, Ma M, Mulder WJM, Fayad Za, Farokhzad OC, Langer R. Mass Production and Size Control of Lipid–Polymer Hybrid Nanoparticles through Controlled Microvortices. Nano Lett. 2012; 12:3587–3591. DOI: 10.1021/nl301253v [PubMed: 22716029]

92. Koh CG, Kang X, Xie Y, Fei Z, Guan J, Yu B, Zhang X, Lee LJ. Delivery of Polyethylenimine/DNA Complexes Assembled in a Microfluidics Device. Mol Pharm. 2009; 6:1333–1342. DOI: 10.1021/mp900016q [PubMed: 19552481]

93. Ling Y, Rubin J, Deng Y, Huang C, Demirci U, Karp JM, Khademhosseini A. A cell-laden microfluidic hydrogel. Lab Chip. 2007; 7:756.doi: 10.1039/b615486g [PubMed: 17538718]

94. Xiao W, He J, Nichol JW, Wang L, Hutson CB, Wang B, Du Y, Fan H, Khademhosseini A. Synthesis and characterization of photocrosslinkable gelatin and silk fibroin interpenetrating polymer network hydrogels. Acta Biomater. 2011; 7:2384–2393. DOI: 10.1016/j.actbio.2011.01.016 [PubMed: 21295165]

95. Fernandez JG, Khademhosseini A. Micro-Masonry: Construction of 3D Structures by Microscale Self-Assembly. Adv Mater. 2010; 22:2538–2541. DOI: 10.1002/adma.200903893 [PubMed: 20440697]

96. Jun Y, Kang E, Chae S, Lee S-H. Microfluidic spinning of micro- and nano-scale fibers for tissue engineering. Lab Chip. 2014; 14:2145.doi: 10.1039/c3lc51414e [PubMed: 24647678]

97. Shin S-J, Park J-Y, Lee J-Y, Park H, Park Y-D, Lee K-B, Whang C-M, Lee S-H. “On the Fly” Continuous Generation of Alginate Fibers Using a Microfluidic Device. Langmuir. 2007; 23:9104–9108. DOI: 10.1021/la700818q [PubMed: 17637008]

98. Lee KH, Shin SJ, Kim C-B, Kim JK, Cho YW, Chung BG, Lee S-H. Microfluidic synthesis of pure chitosan microfibers for bio-artificial liver chip. Lab Chip. 2010; 10:1328.doi: 10.1039/b924987g [PubMed: 20445889]

99. Yamada M, Sugaya S, Naganuma Y, Seki M. Microfluidic synthesis of chemically and physically anisotropic hydrogel microfibers for guided cell growth and networking. Soft Matter. 2012; 8:3122.doi: 10.1039/c2sm07263g

100. Jung J-H, Choi C-H, Chung S, Chung Y-M, Lee C-S. Microfluidic synthesis of a cell adhesive Janus polyurethane microfiber. Lab Chip. 2009; 9:2596.doi: 10.1039/b901308c [PubMed: 19680584]

101. Jeong HH, Lee SH, Lee CS. Fabrication of Janus Microfiber in Microfluidic System. Key Eng Mater. 2011; 493–494:343–348. doi:10.4028/. www.scientific.net/KEM.493-494.343.

102. Marimuthu M, Kim S, An J. Amphiphilic triblock copolymer and a microfluidic device for porous microfiber fabrication. Soft Matter. 2010; 6:2200.doi: 10.1039/b924704a

103. Cheng Y, Yu Y, Fu F, Wang J, Shang L, Gu Z, Zhao Y. Controlled Fabrication of Bioactive Microfibers for Creating Tissue Constructs Using Microfluidic Techniques. ACS Appl Mater Interfaces. 2016; 8:1080–1086. DOI: 10.1021/acsami.5b11445 [PubMed: 26741731]

104. Onoe H, Okitsu T, Itou A, Kato-Negishi M, Gojo R, Kiriya D, Sato K, Miura S, Iwanaga S, Kuribayashi-Shigetomi K, Matsunaga YT, Shimoyama Y, Takeuchi S. Metre-long cell-laden microfibres exhibit tissue morphologies and functions. Nat Mater. 2013; 12:584–590. DOI: 10.1038/nmat3606 [PubMed: 23542870]

105. Tang J, Wang T, Pan X, Sun X, Fan X, Guo Y, Xue H, He J. Synthesis and Electrochemical Characterization of N-Doped Partially Graphitized Ordered Mesoporous Carbon–Co Composite. J Phys Chem C. 2013; 117:16896–16906. DOI: 10.1021/jp405775x

106. Puigmartí-Luis J, Schaffhauser D, Burg BR, Dittrich PS. A Microfluidic Approach for the Formation of Conductive Nanowires and Hollow Hybrid Structures. Adv Mater. 2010; 22:2255–2259. DOI: 10.1002/adma.200903428 [PubMed: 20376849]

107. Huang S, Deshmukh H, Rajagopalan KK, Wang S. Gold nanoparticles electroporation enhanced polyplex delivery to mammalian cells. Electrophoresis. 2014; 35:1837–1845. DOI: 10.1002/elps.201300617 [PubMed: 24777715]

108. Chithrani BD, Ghazani AA, Chan WCW. Determining the Size and Shape Dependence of Gold Nanoparticle Uptake into Mammalian Cells. Nano Lett. 2006; 6:662–668. DOI: 10.1021/nl052396o [PubMed: 16608261]

109. Lazarus LL, Riche CT, Marin BC, Gupta M, Malmstadt N, Brutchey RL. Two-Phase Microfluidic Droplet Flows of Ionic Liquids for the Synthesis of Gold and Silver Nanoparticles. ACS Appl Mater Interfaces. 2012; 4:3077–3083. DOI: 10.1021/am3004413 [PubMed: 22524284]

110. Gupta AK, Gupta M. Synthesis and surface engineering of iron oxide nanoparticles for biomedical applications. Biomaterials. 2005; 26:3995–4021. DOI: 10.1016/j.biomaterials.2004.10.012 [PubMed: 15626447]

111. Abou Hassan A, Sandre O, Cabuil V, Tabeling P. Synthesis of iron oxide nanoparticles in a microfluidic device: preliminary results in a coaxial flow millichannel. Chem Commun. 2008; : 1783.doi: 10.1039/b719550h

112. Abou-Hassan A, Dufrêche J-F, Sandre O, Mériguet G, Bernard O, Cabuil V. Fluorescence Confocal Laser Scanning Microscopy for pH Mapping in a Coaxial Flow Microreactor: Application in the Synthesis of Superparamagnetic Nanoparticles. J Phys Chem C. 2009; 113:18097–18105. DOI: 10.1021/jp9069459

113. Schauermann S, Nilius N, Shaikhutdinov S, Freund H-J. Nanoparticles for Heterogeneous Catalysis: New Mechanistic Insights. Acc Chem Res. 2013; 46:1673–1681. DOI: 10.1021/ar300225s [PubMed: 23252628]

114. Roig Y, Marre S, Cardinal T, Aymonier C. Synthesis of Exciton Luminescent ZnO Nanocrystals Using Continuous Supercritical Microfluidics. Angew Chemie. 2011; 123:12277–12280. DOI: 10.1002/ange.201106201

115. Nightingale AM, de Mello JC. Microscale synthesis of quantum dots. J Mater Chem. 2010; 20:8454.doi: 10.1039/c0jm01221a

116. Liu D, Zhang H, Herranz-Blanco B, Mäkilä E, Lehto V-P, Salonen J, Hirvonen J, Santos HA. Microfluidic Assembly of Monodisperse Multistage pH-Responsive Polymer/Porous Silicon Composites for Precisely Controlled Multi-Drug Delivery. Small. 2014; 10:2029–2038. DOI: 10.1002/smll.201303740 [PubMed: 24616278]

117. Liu D, Zhang H, Mäkilä E, Fan J, Herranz-Blanco B, Wang C-F, Rosa R, Ribeiro AJ, Salonen J, Hirvonen J, Santos HA. Microfluidic assisted one-step fabrication of porous silicon@acetalated dextran nanocomposites for precisely controlled combination chemotherapy. Biomaterials. 2015; 39:249–259. DOI: 10.1016/j.biomaterials.2014.10.079 [PubMed: 25468375]

118. Herranz-Blanco B, Liu D, Mäkilä E, Shahbazi M-A, Ginestar E, Zhang H, Aseyev V, Balasubramanian V, Salonen J, Hirvonen J, Santos HA. On-Chip Self-Assembly of a Smart Hybrid Nanocomposite for Antitumoral Applications. Adv Funct Mater. 2015; 25:1488–1497. DOI: 10.1002/adfm.201404122

119. Hong JS, Stavis SM, DePaoli Lacerda SH, Locascio LE, Raghavan SR, Gaitan M. Microfluidic Directed Self-Assembly of Liposome–Hydrogel Hybrid Nanoparticles. Langmuir. 2010; 26:11581–11588. DOI: 10.1021/la100879p [PubMed: 20429539]

120. Bleul R, Ritzi-Lehnert M, Höth J, Scharpfenecker N, Frese I, Düchs D, Brunklaus S, Hansen-Hagge TE, Meyer-Almes F-J, Drese KS. Compact, cost-efficient microfluidics-based stopped-flow device. Anal Bioanal Chem. 2011; 399:1117–1125. DOI: 10.1007/s00216-010-4446-5 [PubMed: 21116614]

121. Hertzog DE, Michalet X, Jäger M, Kong X, Santiago JG, Weiss S, Bakajin O. Femtomole Mixer for Microsecond Kinetic Studies of Protein Folding. Anal Chem. 2004; 76:7169–7178. DOI: 10.1021/ac048661s [PubMed: 15595857]

122. Gambin Y, Simonnet C, VanDelinder V, Deniz A, Groisman A. Ultrafast microfluidic mixer with three-dimensional flow focusing for studies of biochemical kinetics. Lab Chip. 2010; 10:598–609. DOI: 10.1039/B914174J [PubMed: 20162235]

123. Huang P-H, Nama N, Mao Z, Li P, Rufo J, Chen Y, Xie Y, Wei C-H, Wang L, Huang TJ. A reliable and programmable acoustofluidic pump powered by oscillating sharp-edge structures. Lab Chip. 2014; 14:4319–4323. DOI: 10.1039/C4LC00806E [PubMed: 25188786]

124. Iravani S. Green synthesis of metal nanoparticles using plants. Green Chem. 2011; 13:2638.doi: 10.1039/c1gc15386b

125. Dalwadi. Comparison of Diafiltration and Tangential Flow Filtration for Purification of Nanoparticle Suspensions. Pharm Res. 2005; 22:2152.doi: 10.1007/s11095-005-7781-2 [PubMed: 16151669]

126. Lee BR, Lee KH, Kang E, Kim D-S, Lee S-H. Microfluidic wet spinning of chitosan-alginate microfibers and encapsulation of HepG2 cells in fibers. Biomicrofluidics. 2011; 5:22208.doi: 10.1063/1.3576903 [PubMed: 21799714]

127. De Hazan Y, Wozniak M, Heinecke J, Müller G, Graule T. New Microshaping Concepts for Ceramic/Polymer Nanocomposite and Nanoceramic Fibers. J Am Ceram Soc. 2010; 93:2456–2459. DOI: 10.1111/j.1551-2916.2010.03802.x

128. Hwang CM, Khademhosseini A, Park Y, Sun K, Lee S-H. Microfluidic Chip-Based Fabrication of PLGA Microfiber Scaffolds for Tissue Engineering. Langmuir. 2008; 24:6845–6851. DOI: 10.1021/la800253b [PubMed: 18512874]

129. Thangawng AL, Howell PB Jr, Richards JJ, Erickson JS, Ligler FS. A simple sheath-flow microfluidic device for micro/nanomanufacturing: fabrication of hydrodynamically shaped polymer fibers. Lab Chip. 2009; 9:3126.doi: 10.1039/b910581f [PubMed: 19823729]

130. Nakamura H, Yamaguchi Y, Miyazaki M, Maeda H, Uehara M, Mulvaney P. Preparation of CdSe nanocrystals in a micro-flow-reactor. Chem Commun. 2002; :2844–2845. DOI: 10.1039/b208992k

Biographies

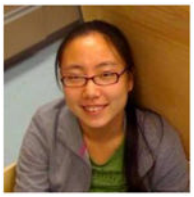

Mengqian Lu received her Bachelor degrees in Theoretical and Applied Mechanics and in Economics from Peking University in China in 2008. She joined the Department of Engineering Science and Mechanics at the Pennsylvania State University as a Ph. D. student in August 2008under the supervision of Professor Tony Jun Huang. She received her in 2014 from the Engineering Science and Mechanics at the Pennsylvania State University.

Adem Ozcelik received his B.Sc. degree in Physics from Karadeniz Technical University, Turkey in 2006. He received his M.S. degree in Materials Science and Engineering and Ph.D. in Engineering Science and Mechanics from The Pennsylvania State University in 2016. Currently, He is working as Postdoctoral Associate in Mechanical Engineering and Materials Science Department at Duke University.

Christopher L. Grigsby received his Ph.D. in Biomedical Engineering from Duke University. He will begin postdoctoral training as a fellow of the Whitaker International

Program at Karolinska Institutet in Stockholm. His research interests include the nanomanufacturing of polymeric gene carriers and their applications in the field of cellular reprogramming.

Yanhui Zhao received his bachelor degree from Zhejiang University at 2006. After that, he joined Institute of Optics and Electronics, Chinese Academy of Sciences for his master studies and graduated at 2009 with a presidential award for his research excellence. He received his Ph.D. in Engineering Science and Mechanics from The Pennsylvania State University in 2014 with his research topics focusing on interdisciplinary research concerning optics, nanotechnology, microfluidics, and fundamental biochemistry.

Feng Guo received his B.S. degree in Physics from Wuhan University, China. In 2011, Feng received his Ph.D. from the Acoustofluidics Lab at the department of Engineering Science and Mechanics, The Pennsylvania State University in 2015. He has been conducting interdisciplinary research in the area of microfluidics, acoustics, cell biology and virology under the guidance of Dr. Tony Jun Huang. His primary research interest is in Acoustic tweezers, specifically, exploring the physics underlying the surface acoustic wave based acoustic manipulation, and applying the acoustic tweezer technology to cell-cell interaction, 3D bio-manufacturing, point-of-care diagnostic instrument.

Kam W. Leong is the Samuel Y. Sheng Professor of Biomedical Engineering at Columbia University, with a joint appointment in the Department of Systems Biology at the Columbia University Medical Center. His research focuses on nanoparticle-mediated drug-, gene- and immuno-therapy, from design of new carriers to applications for cancer, hemophilia, infectious diseases, and cellular reprogramming. He is the Editor-in-Chief of *Biomaterials*, and a member of the National Academy of Inventors and the USA National Academy of Engineering.

Tony Jun Huang is a professor at Department of Mechanical Engineering and Materials Science (MEMS) at Duke University. His research interests are in the fields of acoustofluidics, optofluidics, and micro/nano systems for biomedical diagnostics and therapeutics. He was elected a fellow of the following five professional societies: The American Institute for Medical and Biological Engineering (AIMBE), the American Society of Mechanical Engineers (ASME), the Institute of Electrical and Electronics Engineers (IEEE), the Institute of Physics (IOP), and the Royal Society of Chemistry (RSC).

Highlights

- An overview of recent progress in microfluidic hydrodynamic focusing is presented.
- Distinct designs of flow focusing methods and mechanisms are discussed.
- A future perspective on the key applications and research directions is given.

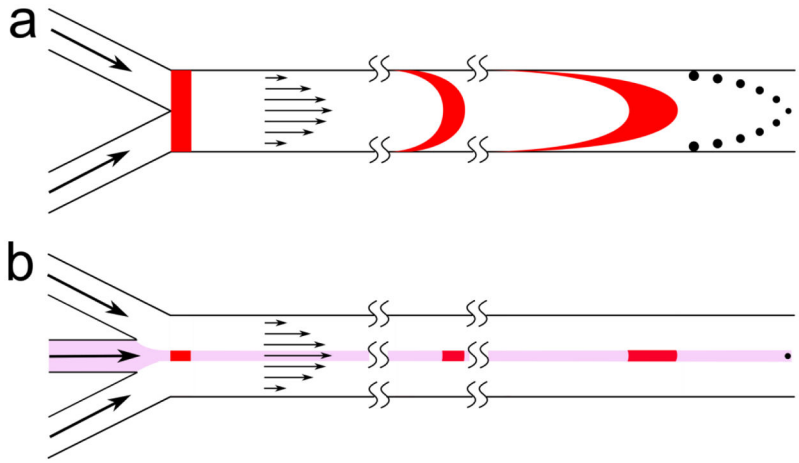

Fig. 1.

The chemical concentration distribution in microfluidic channels. (a) Fluid near the edge of the channel spends longer time in the channel due to the lower velocity resulting in dispersed reaction products within the channel. (b) Hydrodynamic focusing confine the reaction zone to the center of the channel resulting in more uniform reaction time and synthesized product distribution.

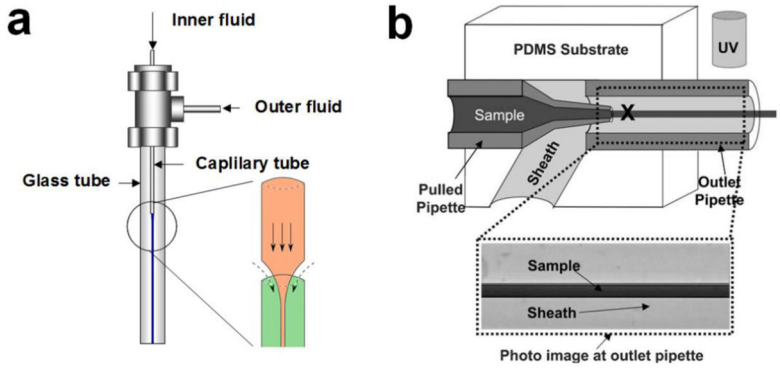

Fig. 2.

Examples of coaxial tube microreactors. (a) Coaxial tube reactor which is an assembly of two concentric capillary tubes [38]. Printed with permission from Elsevier. (b) A coaxial tube reactor assembled by merging pulled glass pipettes with PDMS molding technology [43]. Printed with permission from Royal Society of Chemistry.

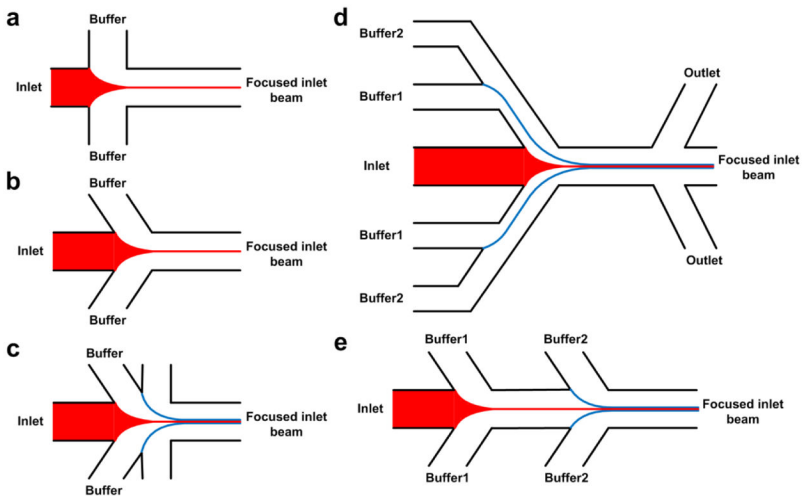

Fig. 3.

Common designs for on-chip HF devices. (a) The central flow is squeezed by two sheath flows from two sides. (b) The sheath-flow channels are tilted to achieve more stable flow profiles (c) Additional sheath-flows are added for improved flow stability and focusing. (d) Bifurcation in the outlets to concentrate the final synthesis products. (d) Multiple HF steps for multi-step synthesis processes.

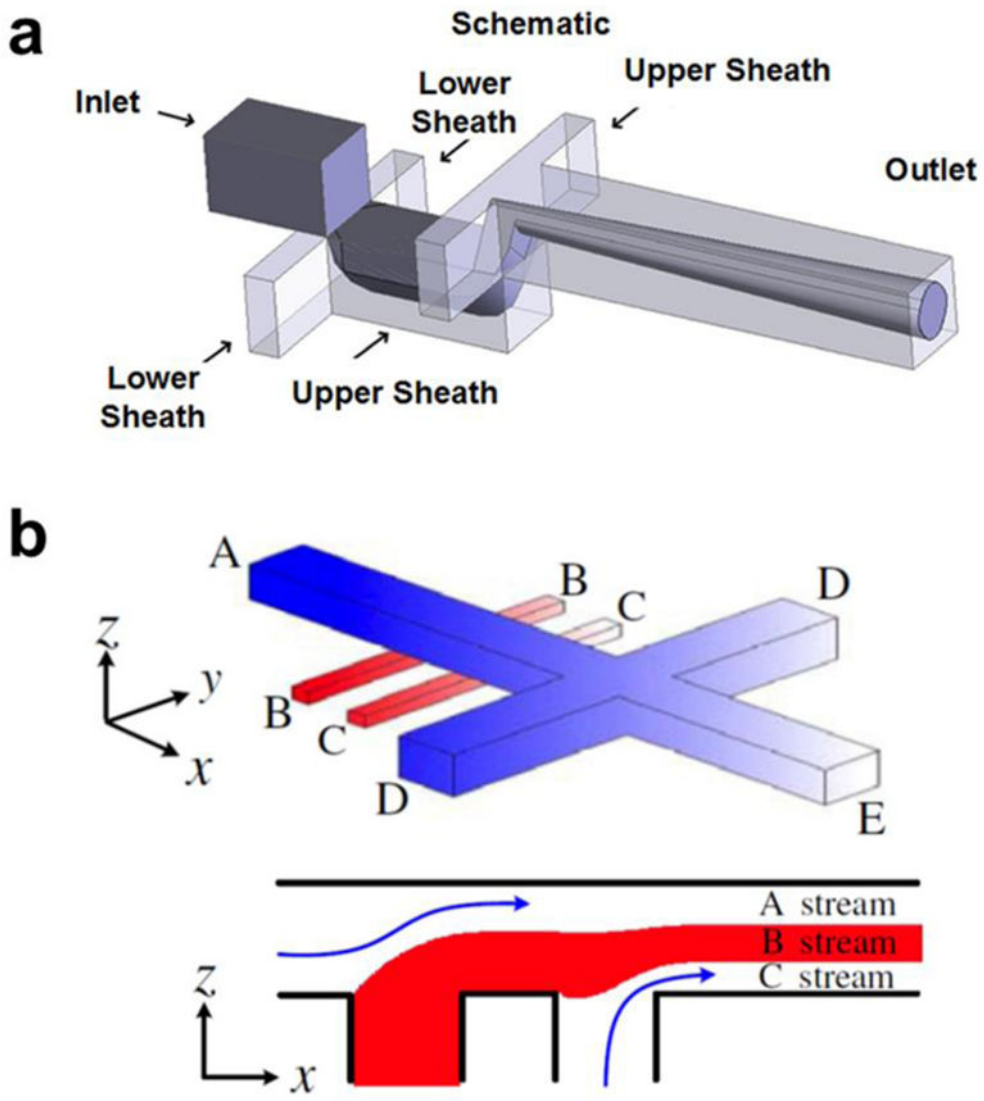

Fig. 4.

Examples of multi-layer on chip 3D HF devices. (a) [88] (Printed with permission from AIP Publishing LLC) and (b) [58] (Printed with permission from IOP Publishing) shows examples of two layer on-chip 3D HF devices utilizing height variations to generate 3D-layered flow structures.

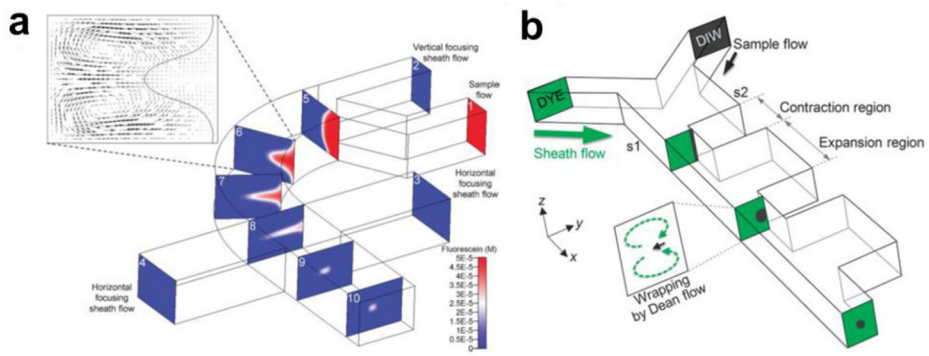

Fig. 5.

Single-layer, planar on-chip devices for 3D HF. (a) “Microfluidic drifting” based 3D HF device [63]. Printed with permission from Royal Society of Chemistry. (b) 3D HF device using counter-rotating vortices generated by a contraction-expansion array [64]. Printed with permission from Royal Society of Chemistry.

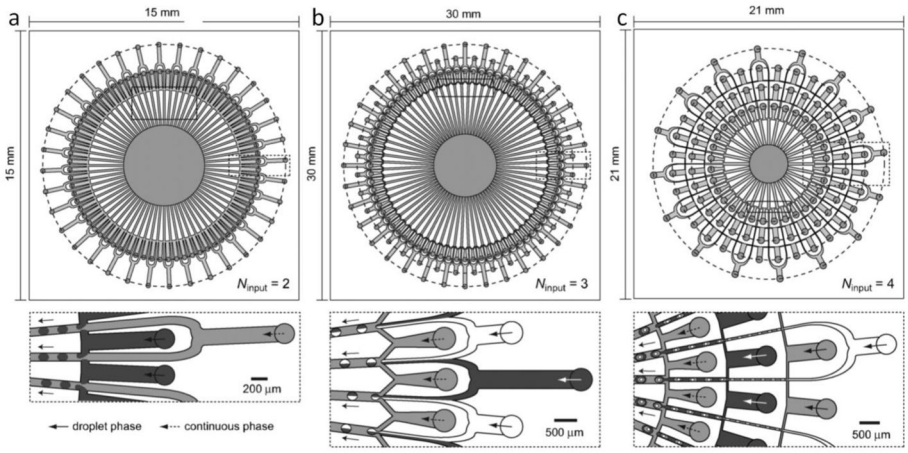

Fig. 6.

An approach to scale-up HF devices for mass production by using multi-array microfluidic modules for (a) single phase, (b) Janus, and (c) core-shell droplet synthesis [68]. Printed with permission from Royal Society of Chemistry.

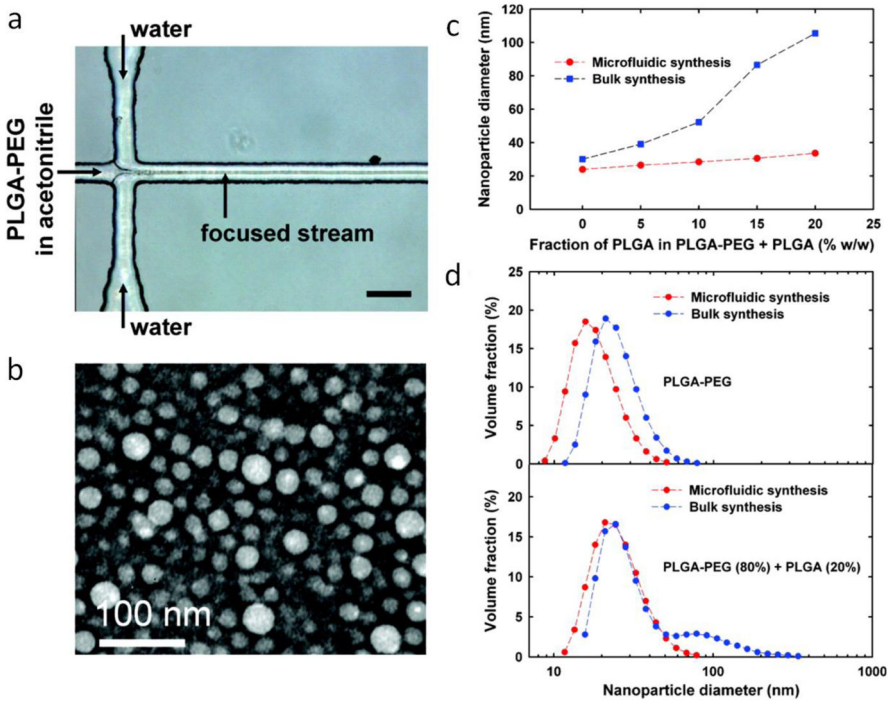

Fig. 7.

Nanoprecipitation of polymer solutions by on-chip HF. (a) PLGA-PEG polymer solution is focused by water sheath flows (scale bar 50 μm). (b) The synthesized polymer nanoparticles show a spherical shape geometry observed by TEM. (c) Compared to the bulk synthesis, on-chip HF yields smaller size nanoparticles at increasing fraction of PLGA in PLGA-PEG solution. (d) In the absence and presence of 20% PLGA, on-chip HF yields a smaller nanoparticle size distribution and no-tail towards the larger diameter nanoparticles, respectively, compared to the bulk synthesis [37]. Printed with permission from American Chemical Society.

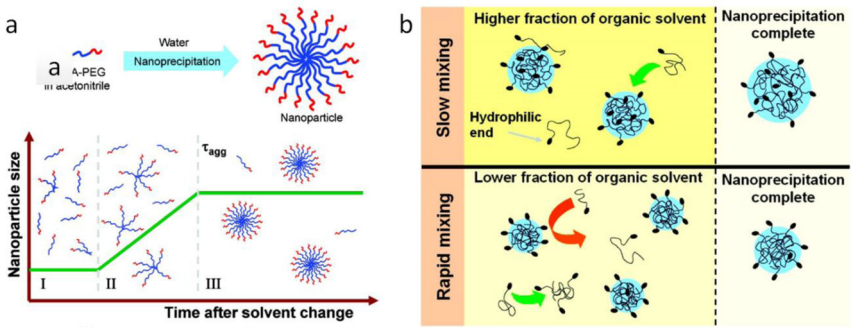

Fig. 8.

Process of polymer nanoprecipitation and the role of mixing time. (a) PLGA-PEG diblock copolymers form into polymer nanoparticles in three stages including (I) nucleation, (II) growth, and (III) nanoparticle formation which is defined by an aggregation time. (b) In the bulk synthesis of PLGA-PEG nanoparticles, slow mixing requires a higher percentage of the organic solvent to initiate nanoprecipitation, and yields larger NP sizes due to easy adsorption of polymers on the growing aggregates. On the other hand, on-chip HF requires lower percentage of the organic solvent to initiate nanoprecipitation by providing rapid mixing preventing excessive polymer adsorption on the aggregates which results in smaller size NPs [37]. Printed with permission from American Chemical Society.

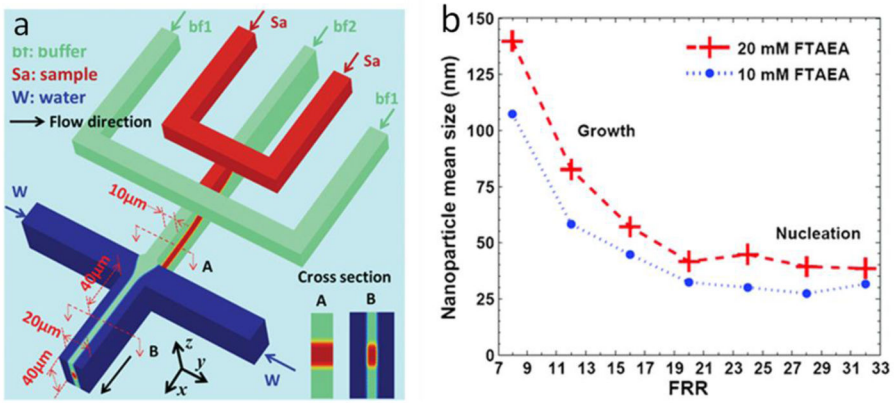

Fig. 9.

Polymer NP synthesis in 3D HF devices. (a) Formation of FTAEA NPs is demonstrated in a 3D on-chip HF device. The Sample stream (Sa) is focused and separated from the channel walls both in vertical and horizontal directions. (b) The ratio of the sheath flows and the sample flow mainly determines the NP mean size as demonstrated at two different initial FTAEA concentrations [81]. Printed with permission from Royal Society of Chemistry.

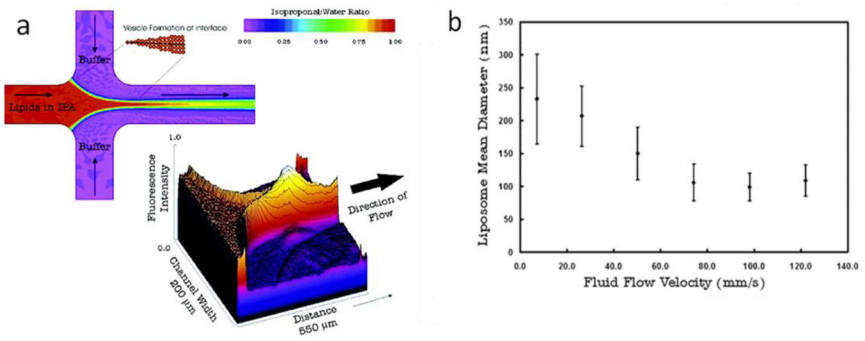

Fig. 10.

Size tunable liposome synthesis in an on-chip HF device by controlling flow rate ratio. (a) a 2D on-chip HF device is utilized to generate nanometers size liposomes through self-assembly of lipids from an isopropyl alcohol (IPA) solution by controlling the IPA/lipid concentration (Contour plot indicates the ratios of the IPA to the buffer solution). (b) The liposome average size is controlled by keeping the IPA + lipid inlet at 2.4 mm/s and increasing the each buffer inlet from 2.4 mm/s to 59.8 mm/s [87]. Printed with permission from American Chemical Society.

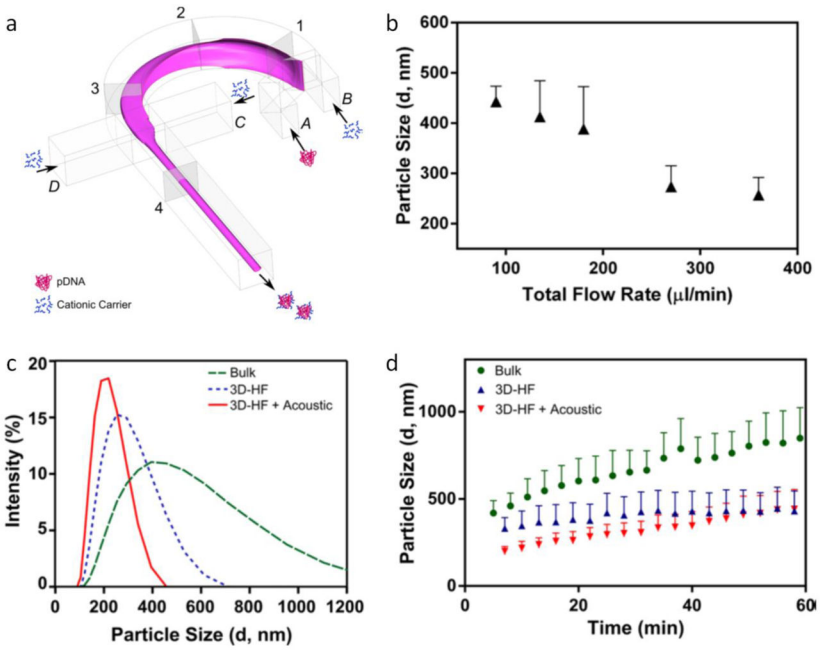

Fig. 11.

Polyplex synthesis in a 3D On-chip HF device. (a) DNA/polymer complexes synthesized by a “microfluidic drifting” based 3D HF device using curved channels and side sheath flows for vertical and horizontal flow focusing, respectively. (b) Diameter of the polyplexes as a function of the total flow rate. (c) Intensity-based size distribution obtained with the reaction using 2 μL Turbofect reagent per μg of pDNA. (d) 3D HF with and without additional gentle acoustic exposure yields less aggregation in time compared to the polyplexes obtained by bulk method [31]. Printed with permission from American Chemical Society.

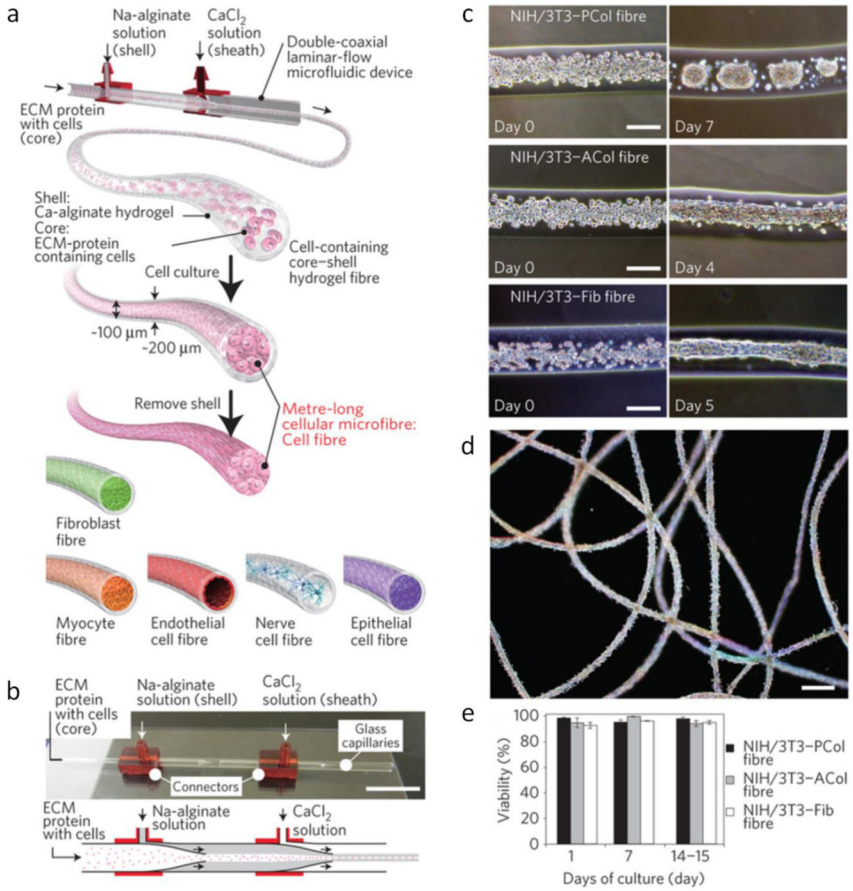

Fig. 12.

Various hydrogel microfibers synthesized by a coaxial HF device [104]. Printed with permission from Nature Publishing Group.

Table 1

Some examples of the organic nanoparticles synthesized by using HF method.

Nanoparticle type	Diameter	Reference
PLGA-PEG copolymers	24 nm	[37]
Polymer-DNA nanocomplexes	263 nm	[31]
poly-2-vinylpyridine-b-poly(ethylene oxide)	40 nm	[80]
Liposomes	50 nm	[85]
Theranostic lipoplexes	194 nm	[86]
Lipid–polymer hybrid nanoparticles	30 nm	[91]
Polyethylenimine/DNA complexes	494 nm	[92]

Table 2

Some examples of the organic fibers synthesized by using HF method.

Fiber type	Diameter	Reference
4-hydroxybutyl acrylate (4-HBA)	35 μm	[43]
Alginate/chitosan	100 μm	[126]
Alginate	19 μm	[97]
4-HBA/PEGDA	15 μm	[127]
PLGA	20 μm	[128]
PMMA	300 μm	[129]
Chitosan	70 μm	[98]
Polyurethane	50 μm	[100]

Table 3

Some examples of the inorganic nanoparticles synthesized by using HF method.

Nanoparticle type	Diameter	Reference
Gold nanoparticles	4.4 nm	[36]
γ-Fe2O3@SiO2 Core/Shell Nanoparticles	50 nm	[46]
Ferrihydrite Nanoparticles	4.1 nm	[45]
TTF–gold nanocomposites	200 nm	[106]
Silver nanoparticles	3.7 nm	[109]
Iron oxide nanoparticles	7 nm	[111]
ZnO nanoparticles	3.5 nm	[114]
CdSe nanocrystals	2 nm	[130]